Biometals (2012) 25:259–273
DOI 10.1007/s10534-011-9500-z

The ferroxidase center is essential for ferritin iron loading in the presence of phosphate and minimizes side reactions that form Fe(III)-phosphate colloids

Robert J. Hilton · N. David Andros · Richard K. Watt

Received: 4 June 2011 / Accepted: 8 October 2011 / Published online: 20 October 2011

Abstract Ferritin iron loading was studied in the presence of physiological serum phosphate concentrations (1 mM), elevated serum concentrations (2–5 mM), and intracellular phosphate concentrations (10 mM). Experiments compared iron loading into homopolymers of H and L ferritin with horse spleen ferritin. Prior to studying the reactions with ferritin, a series of control reactions were performed to study the solution chemistry of Fe^{2+} and phosphate. In the absence of ferritin, phosphate catalyzed Fe^{2+} oxidation and formed soluble polymeric Fe(III)-phosphate complexes. The Fe(III)-phosphate complexes were characterized by electron microscopy and atomic force microscopy, which revealed spherical nanoparticles with diameters of 10–20 nm. The soluble Fe(III)-phosphate complexes also formed as competing reactions during iron loading into ferritin. Elemental analysis on ferritin samples separated from the Fe(III)-phosphate complexes showed that as the phosphate concentration increased, the iron loading into horse ferritin decreased. The composition of the mineral that does form inside horse ferritin has a higher iron/phosphate ratio ($\sim$1:1) than ferritin purified from tissue ($\sim$10:1). Phosphate significantly inhibited iron loading into L ferritin, due to the lack of the ferroxidase center in this homopolymer. Spectrophotometric assays of iron loading into H ferritin showed identical iron loading curves in the presence of phosphate, indicating that the ferroxidase center of H ferritin efficiently competes with phosphate for the binding and oxidation of Fe^{2+}. Additional studies demonstrated that H ferritin ferroxidase activity could be used to oxidize Fe^{2+} and facilitate the transfer of the Fe^{3+} into apo transferrin in the presence of phosphate.

Keywords Non-transferrin bound iron · Ferritin · Chronic kidney disease · Transferrin · Soluble Fe(III)-phosphate complexes · Ferroxidase activity · Ferroxidase assay

R. J. Hilton · N. David Andros · R. K. Watt (✉)
Department of Chemistry and Biochemistry, Brigham Young University, C-210 Benson Building, Provo UT 84602, USA
e-mail: rwatt@chem.byu.edu

Introduction

Chronic kidney disease (CKD) is a chronic inflammatory disease with many altered bio-markers associated with disrupted iron metabolism. These bio-markers include inflammation, non-transferrin bound iron (NTBI), elevated serum ferritin concentrations and low transferrin saturation levels (TSAT) (Prakash et al. 2005; Samouilidou et al. 2007; Stenvinkel and Barany 2002; Kalantar-Zadeh et al. 2006; Lee et al. 2006). The co-existence of NTBI and apo transferrin is puzzling because apo transferrin has a binding constant of $\sim 10^{20}$ (Harris 1986; Baker et al. 2003).

The formation of NTBI in the presence of unsaturated transferrin suggests the presence of either an inhibitor that prevents transferrin from binding iron, or suggests that NTBI is biologically inaccessible to transferrin.

These observations led our group to evaluate conditions that exist in the serum of CKD patients that might allow NTBI to form. The literature reports that phosphate concentrations in serum are significantly elevated (Malluche and Mawad 2002; Tonelli et al. 2010). Patients with CKD have phosphate concentrations reaching concentrations of ~3.5 mM phosphate, which is more than double that of healthy individuals (~1.0–1.5 mM) (Tonelli et al. 2010; Di Marco et al. 2008; Friedman 2005). Phosphate is known to react with iron to produce insoluble complexes (Eq. 1 and 2).

$$3\ Fe^{2+} + 2\ PO_4^{3-} \leftrightarrow Fe_3(PO_4)_2(s) \quad (1)$$

$$K_{sp} = 1.0 \times 10^{-36}$$

$$Fe^{3+} + PO_4^{3-} \leftrightarrow FePO_4(s) \quad (2)$$

$$K_{sp} = 1.3 \times 10^{-22}$$

In addition to the formation of insoluble precipitates, iron, and phosphate react to form soluble polymeric Fe(III)-phosphate complexes when the phosphate concentration is present in excess to the iron concentration (Evans et al. 2008; Rodriguez et al. 2007; Ramanjaneyulu and Shukla 1956). Furthermore, polymeric iron complexes are very poor substrates for donating iron to transferrin (Bates and Schlabach 1975, 1973).

Since polymeric phosphate complexes are poor substrates for loading apo transferrin, it is possible that another protein might be expressed under high phosphate conditions to bind iron. As indicated above, CKD patients have elevated serum ferritin concentrations suggesting a possible role for ferritin as an NTBI binding protein. Also, consistent with this hypothesis are reports that ferritin has increased rates of iron loading in the presence of phosphate (Aitken-Rogers et al. 2004; Orino et al. 2002; Cheng and Chasteen 1991; Polanams et al. 2005; de Silva et al. 1993).

Patients with inflammation contain substantial amounts of iron in serum ferritin (~800 Fe/ferritin) (ten Kate et al. 1997; Herbert et al. 1997) and chronic inflammation patients have serum ferritin levels that are 4–10 fold higher than healthy individuals (Kalantar-Zadeh et al. 2004; Wang et al. 2010; Yamanishi et al. 2002). In addition, inflammation induces the secretion of the H-subunit of ferritin, which possesses the catalytic ferroxidase center required for iron loading. Therefore, the expression and secretion of H ferritin into serum might indicate an attempt to sequester NTBI.

The mechanism for iron loading into serum ferritin is unknown. Iron may be acquired by ferritin during the secretion process as it passes through the endoplasmic reticulum and Golgi apparatus or serum ferritin may acquire iron once it enters the bloodstream (De Domenico et al. 2011; Cohen et al. 2010). The present study was undertaken to evaluate the effectiveness of iron binding by ferritin under serum conditions. We tested ferritin iron loading under physiologically relevant serum phosphate concentrations (~1 mM), elevated serum phosphate concentrations found in CKD patients (~2–5 mM), and for completeness, under cytosolic phosphate concentrations (~10 mM).

We report that elevated phosphate concentrations are inhibitory to iron loading in the predominantly L ferritin rich horse ferritin because of side reactions that form soluble Fe(III)-phosphate complexes. Iron loading into homopolymers of L ferritin was significantly inhibited by phosphate because phosphate binds and oxidizes Fe^{2+} faster than L ferritin is able to bind and oxidize Fe^{2+}. Once the Fe(III)-phosphate complexes form, the iron becomes inaccessible to ferritin. H ferritin can effectively compete with phosphate and prevents or minimizes the side reactions that form Fe(III)-phosphate because the ferroxidase center rapidly binds and oxidizes Fe^{2+}. The ferroxidase activity of H ferritin was able to load apo transferrin with Fe^{3+}, even in the presence of phosphate, demonstrating that ferroxidase activity is not only essential for ferritin loading but may be an important catalyst for transferring iron from ferritin to other iron proteins. These data suggest that under elevated phosphate conditions, the Fe(III)-phosphate complex side reaction may form in vivo and contribute to the pool of NTBI observed in CKD patients.

Experimental procedure

Materials

Equine spleen apo ferritin was purchased from Sigma. Recombinant human heavy chain (rHuH) ferritin from the pET12b HF plasmid and human light chain (rHuL)

ferritin from the pDS20pTrp LF plasmid were generously provided by Paulo Santambrogio (Santambrogio et al. 1993). These plasmids were placed into a BL21-DE3 *E. coli* strain. The rHuH ferritin was grown in LB broth for 8 h at 37°C in a New Brunswick Scientific Bioflo 110 Fermentor/Bioreactor. The rHuL ferritin was grown under the Trp promoter in minimal media M9 broth under similar conditions. Both were purified identically (Santambrogio et al. 1993). H and L ferritin samples were prepared in the apo-form and analyzed for protein and iron content.

Iron loading

Ferritin samples were reconstituted with iron alone or were reconstituted with iron in the presence of phosphate, using the following procedure. An apo ferritin solution (1 μM) was prepared in 0.05 M MOPS buffer, pH 7.4, 0.05 M NaCl. Phosphate was added to the apo ferritin solution to achieve the desired concentration. This solution was stirred aerobically in a cuvette in an Agilent 8453 UV–Vis spectrophotometer and Fe^{2+} ions were added from an anaerobic 0.010 M $FeSO_4$ stock solution to attain the desired iron loading. Typically 100 or 1,000 Fe/ferritin were added so with a protein concentration of 1 μM, a final iron concentration was 100 or 1,000 μM was added to the reaction. Iron loading was monitored spectrophotometrically at 310 nm versus time (Paques et al. 1980; Santambrogio et al. 1996). Control samples with no phosphate or no ferritin were prepared using the identical procedure. Ferritin with higher iron loadings were prepared by adding 100 iron/ferritin in a stirred vial and allowing the iron to incubate with the ferritin for 30 min. This process was repeated until the desired iron/ferritin load was achieved. The spectrum of the resulting samples and control reactions were recorded on the spectrophotometer. The identical procedure was followed for the oxygen electrode assays only the solution was added to the oxygen electrode instead of a cuvette. To remove unbound ions, samples, and controls were passed over a GE Healthcare PD-10 Sephadex G-25 column and the elution profile of these samples and controls were recorded by monitoring the elution peaks at 280 and 310 nm.

Elemental analysis

The following procedure was used to prepare ferritin samples for elemental analysis. After the addition of iron and phosphate, the samples were centrifuged (3,200*g* for 10 min) to remove any precipitated protein or small insoluble complexes. The supernatant (2.0 ml) was treated with 0.5 ml of BioRad Bio-Gel P-10 gel slurry (75 g in 100 ml total volume) and agitated for 30 min. The samples were then centrifuged at (3,200*g* for 10 min) and the supernatant collected. The supernatant was centrifuged through Amicon Ultra–4 centrifugal filters with a 100,000 molecular weight cut-off for 5 min at 3,200*g*. After the first centrifugation step, the concentrated retentate was diluted with 3 ml of 0.05 M MOPS buffer at pH 7.5 with 0.05 M NaCl and centrifuged again. The concentration and dilution steps were repeated two additional times to remove any remaining phosphate in the sample. Finally, the concentrated retentate was resuspended in 1.0 ml of 0.05 M MOPS buffer at pH 7.5 with 0.05 M NaCl.

The iron content of the samples was analyzed by inductively coupled plasma emission (ICP) on a Perkin-Elmer Optima 2000 DV or by formation of the $[Fe(2,2'\text{-bipiridyl})_3]^{2+}$ complex ($\varepsilon_{520} = 8{,}400\ M^{-1}\ cm^{-1}$) after chemical reduction of the iron with sodium dithionite. Protein concentrations were determined using the Lowry Method (Lowry et al. 1951). The phosphate content was measured using a modified phosphomolybdate assay (Fiske and Subbarow 1925) that required the addition of 2% SDS to keep the ferritin protein solubilized. Without the addition of SDS, a blue flocculent precipitate formed that was presumably denatured ferritin as this precipitate did not occur in the absence of ferritin. SDS was shown to solubilize the ferritin precipitate and to have no effect on the standard curve of the assay.

Electron microscopy

Samples were prepared and placed on charged ultra-thin carbon film supported by a lacey carbon film on a 400 mesh copper grid (Ted Pella, Inc.). The grids were charged using a discharge tube to assist in protein binding to the grids. A 3.5 μl sample was incubated on the grid for 30–60 s to allow adherence of the protein or particles to the grid. The liquid was then wicked off, and the grid was rinsed in water. The samples with ferritin were then negative stained by adding 3.5 μl of a 1% solution of uranyl acetate to allow visualization of the protein. Fe(III)-phosphate samples were not stained, as the samples are already electron dense

(iron-containing). The grids were rinsed one more time in water and allowed to dry. The grids were then analyzed using a Tecnai F30 TEM, 140 kV.

Transferrin studies

Human apo transferrin was purchased from Sigma. Apo transferrin (78 kDa) was prepared in a solution of 25 mM MOPS, pH 7.4. $Fe(NH_4)_2(SO_4)_2{\cdot}H_2O$ (Fe^{2+}), $FeCl_3$ (Fe^{3+}), Na_2HPO_4, and $NaHCO_3$, were all purchased from Fisher. Fe^{2+} and Fe^{3+} solutions were prepared by dissolving the appropriate solid into 0.001 M HCl. Nitrilotriacetic acid (NTA) was purchased from Sigma. All solutions were prepared fresh the day they were used.

UV/Vis spectrophotometry

An Agilent 8453 UV/Vis spectrophotometer was used to monitor the binding of iron to transferrin. Final concentrations of protein and solutions were: 5 mg/ml transferrin ($\sim 6 \times 10^{-5}$ M), in 25 mM MOPS buffer pH 7.4, 10 mM CO_3^{2-}, phosphate concentrations as indicated in the figures, and 0.18 mM Fe^{3+} or Fe^{2+}. The kinetic runs were setup to monitor the change in absorbance at 460 nm versus time. Transferrin was combined with carbonate with or without phosphate and allowed to stir to equilibrate. The kinetic run was initiated by adding the appropriate volume of Fe^{3+} or Fe^{2+}. Runs were collected in triplicate. Ferroxidase assays were performed as previously described (Bakker and Boyer 1986). Briefly, 0.5 μM rHuH ferritin was mixed with 60 μM transferrin in 0.025 M MES buffer, pH 6.0, with a final volume of 1.0 ml. An aliquot of two Fe^{2+} atoms per transferrin were added to the solution, with constant stirring. The absorbance change at 460 nm was monitored over time. The oxidation of Fe^{2+} to Fe^{3+} was a result of the ferroxidase center of H chain ferritin. Reactions were performed in the indicated phosphate concentration. All reactions were performed in 10 mM carbonate to provide the appropriate concentration of the synergistic anion for transferrin iron binding.

Results

The following experiments were designed to determine if: (1) phosphate stimulated the rate of iron loading into H, L or horse ferritin; and (2) if ferritin could bind the polymeric Fe(III)-phosphate complexes that may represent NTBI. Experiments were conducted to mimic phosphate concentrations in serum from healthy individuals (1.0 mM), CKD patients ($\sim$3–5 mM) and at intracellular phosphate concentrations (10 mM). Iron loading was monitored by a spectrophotometric assay, oximetry and elemental analysis of the purified samples.

Spectrophotometry/oximetry

The absorbance change at 310 nm is a common assay to monitor iron loading into ferritin (Paques et al. 1980). A second iron loading assay method is to monitor oxygen consumption as Fe^{2+} is oxidized by the ferroxidase center as part of the ferritin iron loading process of ferritin (Yang and Chasteen 1999). The results from both methods are shown in Fig. 1a, b and initial rate data from Fig. 1a, b are represented in Table 1. Data were collected for 0, 1, 5, and 10 mM phosphate, but to simplify Fig. 1, only the data for 1 and 10 mM phosphate are shown to represent the extremes of the range used in this study.

To properly interpret the results from these studies it is essential to understand the solution chemistry of how Fe^{2+} and phosphate react in the absence of ferritin (open symbols in Fig. 1a, b). The first control (open square) shows the slow oxidation of Fe^{2+} to Fe^{3+} in 0.05 M MOPS buffer pH 7.5 in the absence of phosphate or ferritin. The formation of an orange precipitate, $Fe(OH)_3$, confirmed the oxidation of Fe^{2+} to Fe^{3+} in these reactions. When phosphate was present, the initial rate of the reaction increased dramatically in both the UV–Vis reactions (1.0 mM phosphate increased 3.3-fold and 10 mM phosphate increased 13.5-fold) and the oximetry reactions (1.0 mM phosphate increased 2.7-fold and 10 mM phosphate increased 11-fold), compared to the rate of iron oxidation in buffer alone (Table 1). In the presence of phosphate, no visible precipitate was observed, which was surprising considering the K_{sp} values presented in Eq. 1 and 2. The lack of a precipitate and the change in absorbance at 310 nm implied that a soluble Fe(III)-phosphate complex formed and such complexes have been observed previously (Rodriguez et al. 2007; Evans et al. 2008; Ramanjaneyulu and Shukla 1956).

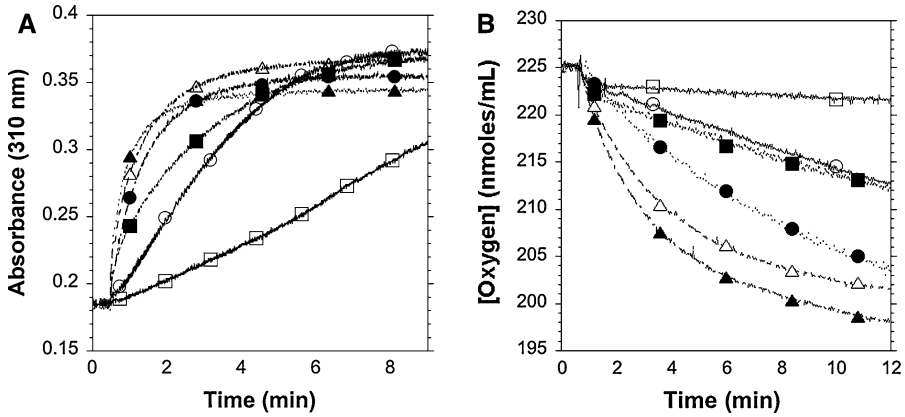

Fig. 1 Ferritin Iron loading Assays. **a** The spectrophotometric assay and **b** the oximetry assay. Each reaction was performed in 0.05 M Mops buffer pH 7.5 and contain no phosphate or the indicated phosphate concentration. Ferritin was present at 1 μM. To start the reaction, Fe^{2+} ions, from an anaerobic 0.01 M $FeSO_4$, were added with a Hamilton syringe to a final concentration of 100 μM to establish a 100 Fe^{2+}/ferritin ratio. Open symbols represent controls without ferritin and closed symbols represent reactions with ferritin. Samples are *open square* Fe(II); *filled square* Fe(II) + ferritin; *open circle* 1 mM phosphate; *filled circle* 1 mM phosphate + ferritin; *open triangle* 10 mM phosphate; *filled triangle* 10 mM phosphate + ferritin

Table 1 Initial rates of iron loading

	Sample	Initial rate (μoles Fe(II) oxidized/sec)	Fold increase
UV/Vis*			
1	Iron added to Mops buffer	0.79 ± 0.08	0
2	1 mM phosphate control	2.6 ± 0.3	3.3
3	10 mM phosphate control	10.7 ± 0.2	13.5
4	Ferritin	3.5 ± 0.4	4.4
5	Ferritin in 1 mM phosphate	11.3 ± 0.3	14.3
6	Ferritin in 10 mM phosphate	22.5 ± 0.6	28.5
Oxygen electrode+			
7	Iron added to Mops buffer	0.4 ± 0.1	0[#]
8	1 mM phosphate control	2.1 ± 0.5	2.7[#]
9	10 mM phosphate control	8.7 ± 0.2	11.0[#]
10	Ferritin	2.3 ± 0.4	2.9[#]
11	Ferritin in 1 mM phosphate	5.9 ± 0.3	7.4[#]
12	Ferritin in 10 mM phosphate	12.6 ± 0.2	15.9[#]

* An apo ferritin solution (1 μM) was prepared in 0.05 M Mops buffer pH 7.4, 0.05 M NaCl. Phosphate was added to the apo ferritin solution to achieve the desired concentration. This solution was stirred aerobically in a cuvette in an Ocean Optics Chem 2000 UV–Vis spectrophotometer and 100 Fe^{2+} ions/ferritin (100 μM final concentration) was added from an anaerobic 0.010 M $FeSO_4$ stock solution. Iron loading was monitored spectrophotometrically at 310 nm versus time. Control samples with no phosphate or no ferritin were prepared using the identical procedure. Initial rates were calculated from the first 20 s of the reaction

+ Identical experimental procedures were used for the oxygen electrode assays

[#] Since the iron only control in the two samples was approximately 50% different, all fold increase calculations were done using the UV/Vis control so the differenced did not vary by 50%

Fe(III)-Pi complex

The results of the control experiments without ferritin indicated that a side reaction occurred that might compete with ferritin during iron loading reactions. Before attempting to interpret the iron loading reaction with ferritin in Fig. 1 and Table 1, further controls were performed to understand Fe^{2+} and phosphate

solution chemistry. The iron and phosphate concentrations were varied to determine when soluble complexes formed and when insoluble Fe(III)-phosphate precipitation reactions occurred. A bluish-green precipitate was observed with a 1:1 Fe^{2+} to phosphate ratio but as the phosphate concentration was increased, less precipitate was observed. When the phosphate concentration was greater than 3-fold, the amount of precipitate decreased significantly and a 10-fold excess of phosphate produced very little precipitate. The phosphate to iron ratios in the assays shown in Fig. 1 are in the range of $\sim$ 20 to $\sim$ 200 phosphate/iron, consistent with the formation of a soluble complex instead of a precipitate (Rodriguez et al. 2007; Evans et al. 2008; Ramanjaneyulu and Shukla 1956).

The spectrum of holo-ferritin, apo ferritin, ferritin prepared with iron in the presence of phosphate and the control without ferritin which formed an Fe(III)-phosphate complex were recorded and are shown in Fig. 2. Apo ferritin shows the typical protein absorbance at 280 nm. Ferritin loaded with iron shows a peak at 280 nm as well as a shoulder trailing into the visible region between 300 and 450 nm, characteristic of iron inside ferritin. The ferritin sample loaded with both iron and phosphate has a similar spectrum as ferritin and iron only, but has a lower absorbance than the ferritin sample from 325 to 450 nm, suggesting that a different mineral with a different extinction coefficient has formed inside ferritin (Polanams et al. 2005). The Fe(III)-phosphate complex that forms independent of ferritin has a peak near 280 nm that trails off into the visible in a similar fashion as ferritin containing iron, but this spectrum has much less absorbance. The spectra show that ferritin containing iron and the Fe(III)-phosphate complex both have significant absorbance at 310 nm. Since this is the wavelength used to monitor the formation of iron in ferritin, the kinetics reported here and in previous works may be monitoring not only the deposition of iron into ferritin but also the formation of the soluble Fe(III)-phosphate complex.

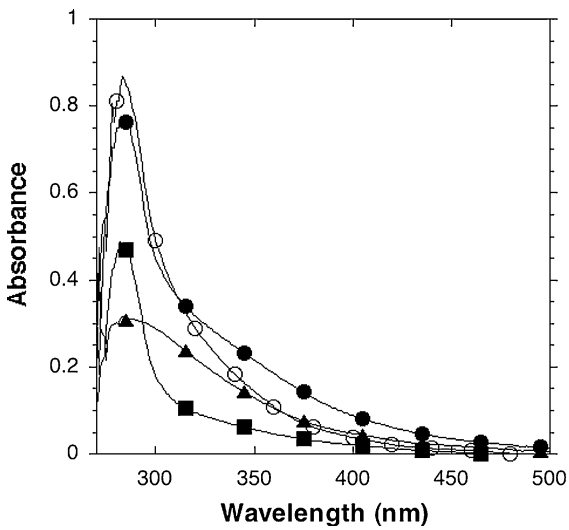

Fig. 2 Spectra of ferritin and Fe(III)-phosphate complex samples. *filled square* apo ferritin, *filled circle* holoferritin, *circle* Ferritin reconstituted by adding Fe(II) to a solution of 1 mM phosphate *filled triangle* the Fe(III)-phosphate complex prepared by adding Fe^{2+} to a 1.0 mM phosphate solution. Samples were prepared to have identical ferritin concentrations (1 μM) and iron concentrations (100 μM). Spectra were recorded after samples were prepared and without any centrifugation steps or separation of unbound ions. This mimics the conditions observed in the kinetic trials

Because an Fe(III)-phosphate complex may form outside of ferritin, the spectrophotometric assay does not confirm that the iron is loading into ferritin. To determine if iron and phosphate were actually loaded into ferritin we developed a method to separate ferritin from the Fe(III)-phosphate complex and performed elemental analysis on the purified ferritin to determine the iron and phosphate content of the samples.

Separating the iron–phosphate complex from ferritin

To determine if the Fe(III)-phosphate complex forms outside of ferritin during iron loading, the following procedure was developed. Ferritin samples and controls were prepared as described for the spectrophotometric assay (Fig. 1) and were centrifuged to remove insoluble material. The supernatant was loaded onto a GE Healthcare PD-10 desalting column. The iron control without ferritin or phosphate precipitated as an orange solid of $Fe(OH)_3$ during the centrifugation step and the supernatant was colorless. When the supernatant of this control was passed over a GE Healthcare PD-10 desalting column, no elution peak was observed, consistent with all of the iron precipitating prior to chromatography (Fig. 3). The ferritin sample prepared in the absence of phosphate had no precipitate after the centrifugation step and eluted in the void volume of the GE Healthcare PD-10 desalting column. Both the 1 and 5 mM phosphate

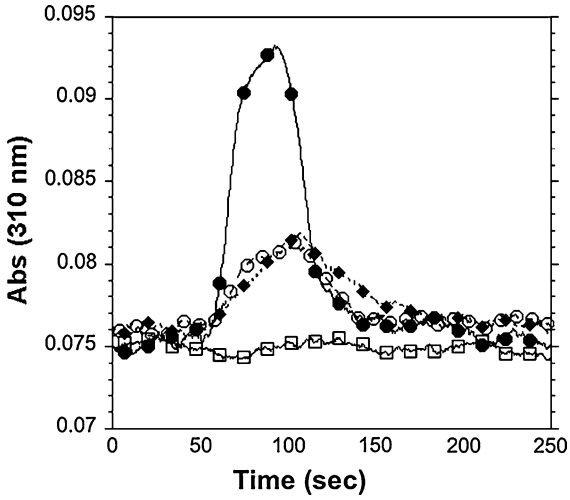

Fig. 3 Gel filtration of ferritin or Fe-phosphate complexes on a GE Healthcare PD-10, G-25 column. *Filled circle* Fe(II) added to apo ferritin, *open circle* Fe(II) added to 1 mM phosphate, *closed diamond*-Fe(II) added to 5 mM phosphate *open square* Fe(II) added to 0.05 M Mops buffer pH 7.5 as a negative control. Identical concentrations were used as those described in Fig. 1. The samples were centrifuged after iron was added to remove insoluble iron precipitates. After centrifugation, the supernatant was loaded onto a GE Healthcare PD-10 column and the eluting species detected as they eluted at 310 nm

controls with iron but no ferritin (representing the Fe(III)-phosphate complex) had very small greenish white pellets but the majority of the iron remained in solution. When the supernatant of these samples was passed over the GE Healthcare PD-10 desalting column, elution peaks were observed near the void volume indicating the presence of large molecular weight species (Fig. 3). Ferritin, with a molecular mass of ~450,000 Da, should clearly separate from Fe^{2+}, Fe^{3+}, or phosphate if they exist as ions or small complexes. The results from the PD-10 column suggest that a large molecular mass Fe(III)-phosphate complex is formed.

Centrifugal filter devices were also used to confirm that the Fe(III)-phosphate controls formed large molecular weight species. Control samples were prepared by adding Fe^{2+} to solutions containing 1 or 5 mM phosphate. These samples were incubated for the appropriate amount of time to compare with the samples prepared in Fig. 1. The solutions were loaded onto Amicon Ultra centrifugal filter devices with a molecular weight cut-off of 100 kDa. After centrifugation, the retentate and the flow-through were analyzed for iron by the addition of 2-2′-bipyridyl, which specifically chelates Fe^{2+}. Neither the flow-thru nor retentate changed color upon α-α′-bipyridyl addition, indicating that the Fe^{2+} ions had been oxidized to Fe^{3+} (Harris and Aisen 1973; Evans et al. 2008). When the reductant sodium dithionite was added to both chambers, the flow-through remained colorless but the retentate turned red, indicating that the Fe(III)-phosphate complex was large and did not pass through the 100 kDa filters. These data are consistent with the results from the GE healthcare PD-10 column (Fig. 3) and indicate that the Fe(III)-phosphate complex is large. The results also show that iron is in the Fe(III) oxidation state.

The Fe(III)-phosphate complex was separated from ferritin using a BioRad P-10 Gel. A 2.5 × 15 cm column of BioRad P-10 was prepared and equilibrated with 0.05 M Mops buffer pH 7.5 with 0.05 M NaCl. Ferritin passed through the column, whereas the Fe(III)-phosphate complex bound tightly to the column. The Fe(III)-phosphate complex is released from the BioRad P-10 resin by passing an anaerobic solution of 1 mM sodium dithionite and 0.5 mM bipyridyl, which chemically reduces and chelates the iron. Any remaining free phosphate could be removed from the ferritin samples by passing the sample over a GE Healthcare PD-10 column or by repeated concentration and dilution using an Amicon Ultra centrifugal filter system as described in "Materials". Subsequent experiments showed that 0.5 ml of 70% BioRad P-10 slurry in water added to 2.0 ml of sample specifically and quantitatively bound the Fe(III)-phosphate complex. This procedure provided a convenient method to rapidly remove Fe(III)-phosphate complexes from solution and permitted elemental analysis to be performed on ferritin samples. Samples prepared by removing the Fe(III)-phosphate complex using the BioRad P-10 column or by using the batch BioRad P-10 precipitation method gave the same results by elemental analysis, confirming the effectiveness of the latter method.

Preliminary characterization of this complex shows a polynuclear complex with a ratio around two irons to three phosphates. Gel filtration experiments (Fig. 3) show the complex is large. Electron microscopy of the sample compares ferritin particles that are 12 nm in diameter (Fig. 4a) with the polynuclear Fe(III)-phosphate complex that forms particles ranging from 10 to 20 nm in diameter by EM (Fig. 4b). The same solutions were incubated for about a week and

analyzed by Atomic Force Microscopy (AFM). Ferritin particles were observed as monomers, dimers, and tetramers (Fig. 4c) and Fe(III)-phosphate particles were observed to have larger sizes with 10–200 nm diameters in the AFM (Fig. 4d). The larger sized particles are presumed to form by particle aggregation that occurred in solution during the weeklong incubation. Since the phosphate protonation at pH 7.5 is a mixture of HPO_4^{2-} and $H_2PO_4^-$, changes in pH will be important in how much of this complex forms. A careful characterization of the stoichiometry, pH of formation and size of this complex as well as reactivity toward catalyzing the formation of reactive oxygen species is underway in our laboratory.

Iron loading into ferritin

Once conditions were established to separate the Fe(III)-phosphate complex from ferritin, elemental analysis was performed. The data from the elemental analysis (Table 2) was compared to the analysis of the initial rates of the UV/Vis and oximetry assays (Table 1) to understand iron loading into ferritin and when the Fe(III)-phosphate complex formed. Scheme 1 summarizes the data shown in Fig. 1 and Tables 1, 2 and represents the reactions that are occurring under these conditions.

The initial rate of the reaction of Fe^{2+} with ferritin in the presence of physiological concentrations of phosphate (1 mM) was measured in the spectrophotometric assay to be 3.25-times faster than ferritin iron loading without phosphate (compare lines 4 and 5 in Table 1) and is 4.3-times faster than the control of 1 mM phosphate control without ferritin present (compare lines 2 and 5 in Table 1). These data show that with normal serum phosphate concentrations (1.0 mM), ferritin appears to load faster than without phosphate. Table 2 shows the actual deposition of the iron in ferritin and shows that ~67 and 75% of the iron was incorporated when 100 and 1,000 iron atoms were loaded into

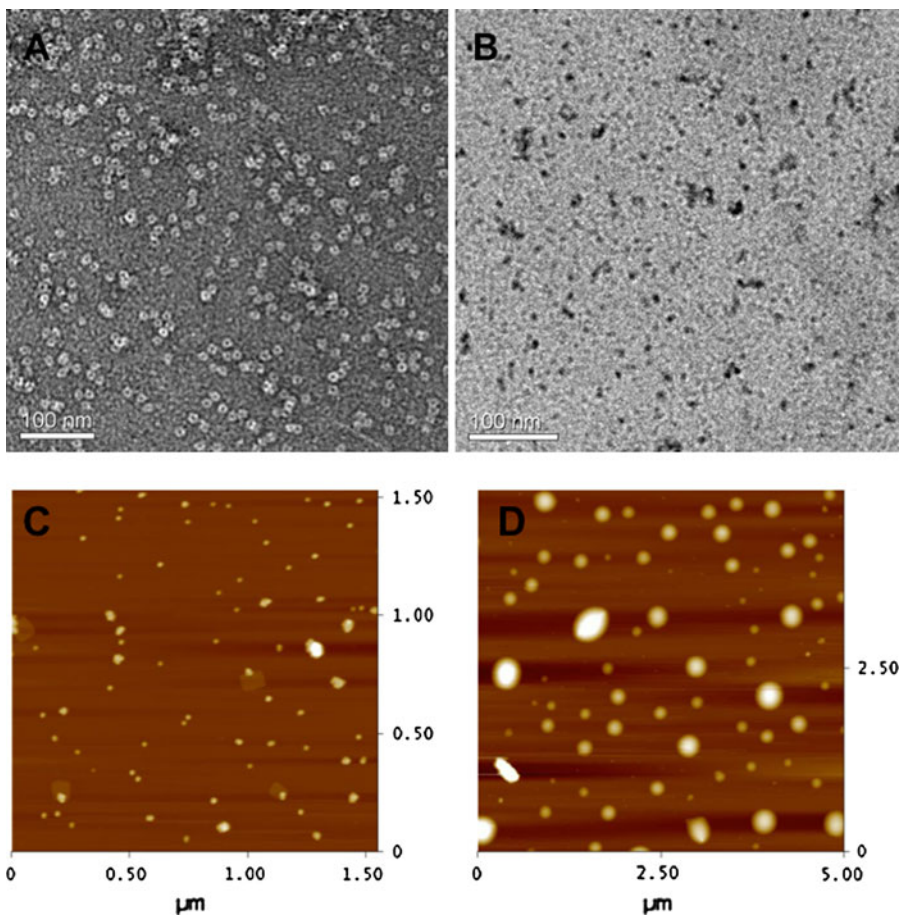

Fig. 4 Electron micrographs and AFM of ferritin and Fe(III)-phosphate complexes. **a** EM images of ferritin that were *negative stained* with uranyl acetate to show the protein shell, compared to **b** *non-stained* Fe(III)-phosphate complexes. Atomic force micrographs are shown of **c** ferritin and **d** the Fe(III)-phosphate complex. The Fe(III)-phosphate complex was formed as described in "Materials" and in Figs. 1 and 2 and the supernatant was placed on an EM or AFM grid

Table 2 Elemental analysis

Theoretical loading	Iron/ ferritin	Phosphate/ ferritin	Iron/ phosphate
100 Iron/ferritin			
No phosphate	119 ± 7	5.3 ± 0.4	24 ± 2
1 mM phosphate	67 ± 6	35.1 ± 1.2	2.0 ± 0.2
2.5 mM phosphate	54 ± 2	51.1 ± 0.6	1.1 ± 0.04
5 mM phosphate	33 ± 3	25.1 ± 1.4	1.4 ± 0.14
10 mM phosphate	25 ± 3	3.85 ± 0.5	6.6 ± 1.7
1,000 Iron/ferritin			
No phosphate	1069 ± 26	5.1 ± 0.4	210 ± 17
1 mM phosphate	752 ± 38	582 ± 24	1.3 ± 0.08
2.5 mM phosphate	692 ± 13	318 ± 19	2.1 ± 0.13
5 mM phosphate	232 ± 36	356 ± 67	0.7 ± 0.17
10 mM phosphate	84 ± 11	83 ± 20	1.01 ± 0.28

ferritin, respectively. Similar results are observed by comparing the corresponding reactions for the oximetry data (Table 1). The phosphate controls are very close between the UV/Vis reactions and the oximetry reactions. However, the rates and fold increases between the UV/Vis and oximetry assays vary by a factor of two. This can be explained by the method of detection. The UV/Vis reaction measures the absorbance change at 310 nm to detect the oxidation of 2 Fe(II) ions that form an Fe(III) oxo dimer ($\varepsilon = 3540\ M^{-1}\ cm^{-1}$ for the Fe(III) dimer) (Yang et al. 2000). As the Fe(III) migrates to the core, the core also has an absorbance that contributes to the UV/Vis spectrum ($\varepsilon = 2285\ M^{-1}\ cm^{-1}$ for the dimer) (Yang et al. 2000). Therefore, the initial rates and fold increases shown in the ferritin samples studied by the UV/Vis assay are approximately double the values shown for the oximetry data. Since the oximetry date is only measuring the oxygen consumption at the ferroxidase center, these results are probably the most accurate.

The increased rate of iron loading with phosphate and ferritin is consistent with previous studies indicating that phosphate stimulates the reaction rate at the ferroxidase center. The higher percentage of iron loading in the larger core is consistent with data showing that phosphate on the mineral core surface assists iron binding and oxidation (Xu and Chasteen 1991).

The reaction of ferritin in 10 mM phosphate in the spectrophotometric assay showed the fastest initial rate and is ~2-times faster than the 1 mM phosphate reaction with ferritin present (compare lines 5 and 6 in Table 1) but was only ~2 times faster than the 10 mM phosphate control without ferritin (compare lines 3 and 6 in Table 1). The elevated phosphate concentration improves the collision frequency of phosphate with Fe^{2+} in solution and allows the formation of an Fe(II)-phosphate complex that rapidly oxidizes to form the Fe(III)-phosphate complex. This competition and depletion of free Fe^{2+} minimizes the amount of iron that loads into ferritin. This is confirmed in Table 2 where iron loading into ferritin is significantly inhibited by the presence of 10 mM phosphate. This could be anticipated by comparing the reaction profile curves for 10 mM phosphate and 10 mM phosphate and ferritin in Fig. 1. The curves almost overlap, indicating that the Fe(III)-phosphate complex formation is very favorable under these conditions. As before, the oximetry data is consistent with the spectrophotometric assay.

The Fe(III)-phosphate complex is not a substrate for loading iron into ferritin. All attempts to use the pre-formed Fe(III)-phosphate complex as a substrate for iron loading into apo ferritin, including various reaction times were unsuccessful. Attempts to modify the work by Levi et al. using ascorbic acid as a reducing agent to reduce the Fe(III)-phosphate complex were also unsuccessful indicating that ascorbic acid is not a sufficiently strong reducing agent to reduce the Fe(III)-phosphate complex (Levi et al. 1996). Even with a large excess of iron, no more than a few iron(III) ions (~10/ferritin) could be loaded into ferritin using ascorbic acid and the Fe(III)-phosphate complex. We conclude that under the conditions used, the Fe(III)-phosphate complex is not a substrate for loading iron into ferritin.

Fe(III)-phosphate mineralization in ferritin

Samples were prepared at two levels of iron loading: 100 iron/ferritin and 1,000 iron/ferritin. The phosphate concentrations present during iron loading were 1, 2.5, 5, and 10 mM. Table 2 shows that when iron was added in the absence of phosphate, essentially all of the iron was incorporated into ferritin at both the low (100 iron/ferritin) and high (1,000 iron/ferritin) samples. When the physiological concentration of serum

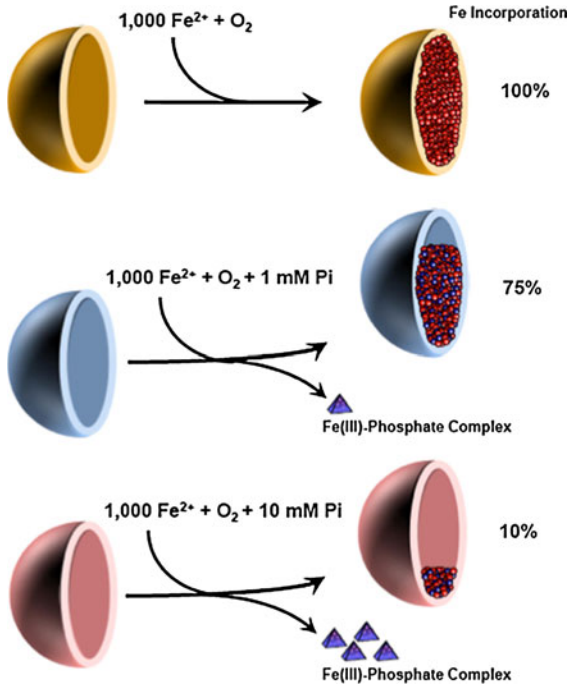

Scheme 1 Iron loading into horse spleen ferritin. In the absence of phosphate, iron loading into ferritin is very efficient with essentially all of the iron sequestered inside ferritin (*top panel*). Iron loading under physiologically normal phosphate concentrations (1 mM) produce ferritin with approximately 75% of the iron sequestered in ferritin but about 25% of the iron is diverted to the side reaction forming the Fe(III)-phosphate complex (*middle panel*). When reactions are performed in phosphate concentrations that would be found in CKD patients (3.5 mM) or in the cytosol (10 mM), iron loading into ferritin is prevented by the formation of the Fe(III)-phosphate complex

phosphate (1 mM) was used, the efficiency of iron loading into ferritin decreased and ranged between 67 and 75% depending on the core size. At 2.5 mM phosphate, approximately 50% of the iron deposited in the 100 Fe/ferritin sample and ~70% in the 1,000 iron/ferritin samples. When 5 mM phosphate was present, iron loading was very poor with approximately 20–30% of the iron loaded into ferritin, leaving 70–80% of the iron unbound by ferritin. Finally, 10 mM phosphate showed ~90% inhibition of iron loading into ferritin. At the lower phosphate concentrations, it appears that as the core gets larger, the efficiency of ferritin to bind and sequester iron improves (compare 1 and 2.5 mM for 100 and 1,000 Fe/ferritin). This effect is probably due to the autocatalytic iron binding and oxidation properties of the iron mineral core (Sun and Chasteen 1992). As the phosphate concentration increases, the larger amount of iron added to ferritin is less efficiently bound by ferritin. This suggests that at higher phosphate concentrations, the formation of the Fe(III)-phosphate complex dominates the binding of iron. This suggests that the early steps in core formation are critical for efficient iron loading into ferritin in the presence of phosphate.

To test the hypothesis that the early steps in core formation are critical for iron loading into ferritin in the presence of phosphate, iron loading was performed with both H ferritin, possessing the ferroxidase center, and L ferritin, possessing the nucleation site. The H-subunit has a ferroxidase center and will initiate the formation of a core much faster than L ferritin, which relies on Fe^{2+} diffusing into the interior of the core and binding at the nucleation site and oxidizing at that location to initiate a core.

Recombinant H and L ferritins

In order to better understand the effects of the ferroxidase center (H ferritin) and the nucleation centers (L ferritins), we used recombinant human H ferritin (rHuH) and recombinant human L ferritin (rHuL), and repeated the above iron loading experiments with and without phosphate. Figure 5 shows iron loading into H and L ferritins in the presence and absence of phosphate. The presence or absence of phosphate did not alter the rate of iron loading into H ferritin using the spectrophotometric assay (Fig. 5a). Elemental analysis of samples prepared in 1–10 mM phosphate showed less than a 10% difference in total iron loading as phosphate increased. This suggests that the ferroxidase center of H chain ferritin is capable of oxidizing and sequestering iron faster than phosphate, thus out-competing phosphate for Fe^{2+}. However, with L ferritin, the spectrophotometric assay shows that the rate of the reaction is much slower but appears to be stimulated in the presence of increasing phosphate concentrations (Fig. 5b). Controls in the absence of ferritin show identical reaction curves to L ferritin, indicating that the reaction observed in this assay is the formation of the Fe(III)-phosphate complex. Elemental analysis confirmed this by showing that even in 1 mM phosphate, only about 10% of the added Fe^{2+} was sequestered inside L ferritin. Without a ferroxidase center, L ferritin cannot compete with phosphate for binding and oxidizing Fe^{2+} and essentially all of the added Fe^{2+} ions react with phosphate and are oxidized to form the Fe(III)-phosphate complex.

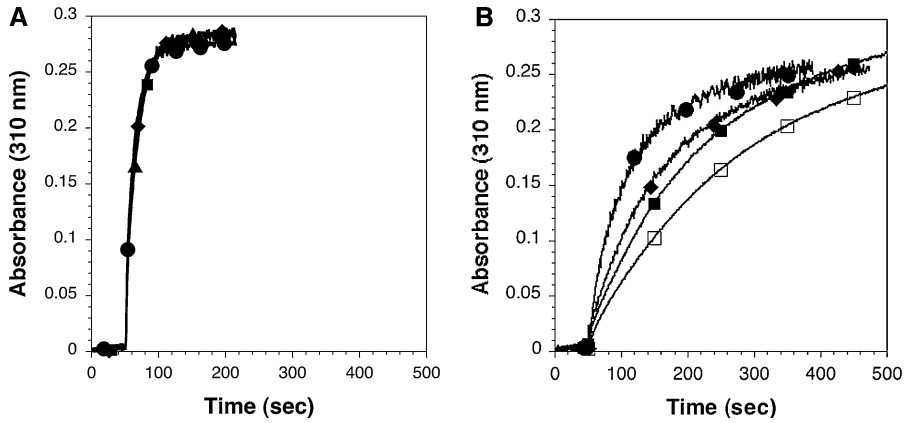

Fig. 5 Iron loading into rHuH and rHuL ferritins in the presence and absence of phosphate. Ferritin was present at 1 μM. To start the reaction, Fe^{2+} ions, from an anaerobic 0.01 M $FeSO_4$, were added with a Hamilton syringe to a final concentration of 100 μM to establish a 100 Fe^{2+}/ferritin ratio. **a** rHuH ferritin in the absence of phosphate (*filled triangle*) and with (*filled square*) 2.5 mM, (*filled diamond*) 5.0 mM and (*filled circle*) 10 mM phosphate. **b** rHuL ferritin in the absence of phosphate (*open square*) and with 2.5 mM (*filled square*), 5.0 mM (*filled diamond*) and 10 mM phosphate (*filled circle*). Note that the rHuH (**a**) and rHuL (**b**) ferritin samples are plotted on the same time axis to emphasize the differences in reaction rates between the two samples

The ability of H ferritin to rapidly oxidize Fe^{2+} may have significance in vivo by providing ferroxidase activity for iron storage or for loading iron onto other proteins. As an iron storage protein, it is logical that iron-requiring proteins might interact with ferritin to obtain iron. In general, Fe^{2+} is more mobile because of faster ligand exchange rates for Fe^{2+}. In contrast Fe^{3+} has much slower ligand exchange rates and is relatively immobile. The ferroxidase center may play an essential role in oxidizing Fe^{2+} as it is transferred to other proteins to ensure that the released iron is stabilized in the accepting protein. The original ferroxidase assay demonstrated that ferritin was capable of oxidizing Fe^{2+} to Fe^{3+} for iron incorporation into apo transferrin (Bakker and Boyer 1986). Similar iron deposition reactions are catalyzed in vivo by ferroportin and ceruloplasmin (De Domenico et al. 2007). To be a functional iron release mechanism, such a process must occur under physiological phosphate conditions. Therefore, we tested H ferritin for the ability to load apo transferrin in the presence of varying concentrations of phosphate. Figure 6a shows the rate of iron loading into apo transferrin by monitoring the increase in absorbance at 460 nm that corresponds to the formation of diferric transferrin in the absence and presence of phosphate. The control shows the slow auto-oxidation of Fe^{2+} in the absence of ferroxidase activity. It is evident that H ferritin on its own is capable of accelerating the rate of Fe^{2+} oxidation and incorporation of Fe^{3+} into apo transferrin. The addition of 1.0, 2.5, 5, and 10 mM phosphate to this reaction caused an increase in the initial rate of apo transferrin loading, indicating that the phosphate stimulates the rate of Fe^{2+} oxidation at the H ferritin ferroxidase center as previously reported (Orino et al. 2002; Aitken-Rogers et al. 2004; Cheng and Chasteen 1991; Polanams et al. 2005). However, above 2.5 mM phosphate, the final absorbance begins to decrease, indicating that at these higher phosphate concentrations, the formation of the Fe(III)-phosphate complex begins to compete with H ferritin for the added Fe^{2+}. To confirm that the reaction is really catalyzed by H ferritin, and that phosphate is stimulating the activity of the H ferritin ferroxidase activity, controls in the absence of H ferritin were performed. Figure 6b compares the rate of Fe^{3+} binding to apo transferrin in the presence and absence of H ferritin at corresponding phosphate concentrations. In each case, H ferritin is faster than phosphate alone. In addition, for the higher phosphate concentrations, the final absorbance is much higher for the H ferritin reaction, indicating that the H ferritin allowed more iron to be loaded into apo transferrin.

Discussion

The present study demonstrated that phosphate inhibited iron loading into horse ferritin and homopolymers of L ferritin through a competing side reaction that

produced a soluble Fe(III)-phosphate complex. Once formed, the Fe(III)-phosphate complex was not a substrate for loading into H, L or horse ferritin. In contrast to L ferritin, H ferritin can efficiently bind, oxidize, and sequester Fe^{2+} in the presence of phosphate. Since serum ferritin is reported to be predominantly L ferritin, serum ferritin would be unable to bind, oxidize and sequester free Fe^{2+} in the bloodstream (Arosio et al. 2009). However, the expression and secretion of H ferritin during inflammation may be a response to provide the appropriate catalytic H chain ferritin subunits to bind and sequester free Fe^{2+} when serum phosphate levels increase. These results also explain why cytosolic ferritins form heteropolymers of both H and L subunits because the ferroxidase center of the H ferritin is required to outcompete phosphate in order to sequester Fe^{2+}. These results are also consistent with reports that the overexpression of L homopolymers in bacteria results in the formation of apo ferritin (Levi et al. 1989). Furthermore, the complexation of iron by phosphate may not be limited only to phosphate but may include other cytosolic molecules capable of complexing iron. During the early characterization of the H and L homopolymers, Santambrogio et al. demonstrated that phosphate and citrate completely inhibited iron loading into L homopolymers (Santambrogio et al. 1996).

Elemental analysis on purified horse ferritin samples showed that phosphate was inhibitory to iron loading in predominantly L ferritin and that phosphate concentrations observed in CKD patients ($\sim$3.5 mM) blocked $\sim$50% of the available Fe^{2+} from entering ferritin (Table 2). If this occurs in vivo, a change from healthy phosphate levels (1.0 mM phosphate) to levels measured in CKD patients ($\sim$3.5 mM) could cause a doubling in the amount of free iron, or NTBI in serum.

Native ferritin is commonly reported to contain approximately ten iron atoms per phosphate, but studies using density gradient centrifugation showed that ferritin with more phosphate exist in a heterogeneous sample (Juan and Aust 1998). However, in vitro iron loading in the presence of phosphate produced cores with a 1:1 iron to phosphate ratio, which is very different than native ferritin cores (Table 2). Several groups have prepared native-like mineral cores ($\sim$ 10 Fe/phosphate) in ferritin by first loading the iron and then incubating ferritin in a phosphate solution (Treffry and Harrison 1978; de Silva et al. 1993). It was proposed that to obtain ferritin samples with the low phosphate contents found in vivo ferritin

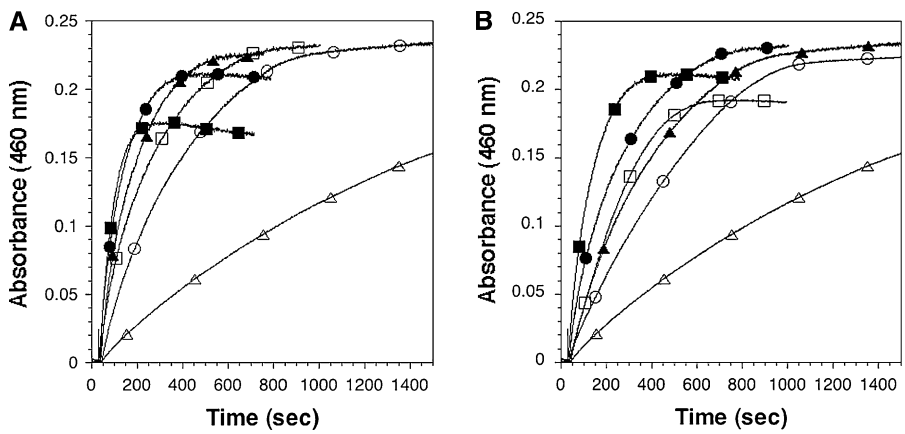

Fig. 6 The ferroxidase assay in the presence and absence of phosphate. rHuH ferritin was used to oxidize Fe^{2+} to Fe^{3+} to load iron into apo transferrin. **a** Fe^{2+} oxidation in the (*open triangle*) absence of rHuH ferritin and (*open circle*) in the presence of rHuH ferritin to load apo transferrin. Other reactions include rHuH ferritin in the presence of phosphate at concentrations of (*open square*) 1.0 mM, (*filled triangle*) 2.5 mM, (*filled* circle) 5 mM, and (*filled square*) 10 mM phosphate. **b** Comparison of ferroxidase assay shown in Fig. 6a with controls that do not contain rHuH ferritin but have the same phosphate concentrations. Open symbols represent samples with no H ferritin but the corresponding filled symbol represents the same phosphate concentration with H ferritin. The samples are (*open triangle*) no phosphate and no rHuH ferritin (auto-oxidation), (*filled triangle*) no phosphate but rHuH ferritin, (*open circle*) 1.0 mM phosphate with no rHuH ferritin, (*filled circle*) 1.0 mM phosphate with rHuH ferritin, (*open square*) 5 mM phosphate with no rHuH ferritin, and (*filled square*) 5 mM phosphate with rHuH ferritin

would be required to dock with a membrane ion transport protein to allow iron to be directly channeled into ferritin followed by phosphate deposition on the mineral surface. Another proposal suggested that ferritin is sequestered in a protected environment where phosphate was not available during iron loading. Early ferritin iron loading studies were conducted in liver extracts and produced ferritin mineral cores that differed from purified ferritin loaded in vitro (Granick and Hahn 1944). To explain this difference, Granick suggested the presence of a specific enzyme required for this metabolic synthesis of an "iron micelle" into ferritin (Granick and Hahn 1944). Recently, an intracellular iron-chaperone protein was discovered (Shi et al. 2008). This iron-chaperone protein, named PCBP1, corresponds to a family of RNA binding proteins belonging to the heterogeneous nuclear ribonucleoprotein K-homology domain superfamily. PCBP1 binds to ferritin in the presence of Fe^{2+} and increases the loading of ferritin both in vivo and in vitro. A serum analog of PCBP1 has not yet been identified but is an intriguing possibility for serum ferritin iron loading.

Phosphate has been reported to stimulate the rate of iron loading into ferritin (Orino et al. 2002; Aitken-Rogers et al. 2004; Polanams et al. 2005; Cheng and Chasteen 1991). Phosphate may interact at or near the ferroxidase center to shift the redox potential for oxidation, it may assist in the migration of iron into the core or may bind on the core surface and act as a ligand for incoming iron (Cheng and Chasteen 1991; Aitken-Rogers et al. 2004; Johnson et al. 1999). Our results are consistent with the above data showing that in 1 mM phosphate the rate of Fe^{2+} oxidation is a $\sim$ 3-fold faster than ferritin without phosphate (Table 1). The ferroxidase assay loading iron into apo transferrin further demonstrated that H ferritin catalyzed iron loading into apo transferrin more rapidly when phosphate was present (Fig. 6).

In summary, phosphate stimulates the activity of the ferroxidase center of H ferritin. The discovery that a soluble Fe(III)-phosphate complex forms as a competing side reaction during iron loading into ferritin has significant implications on how iron loads into ferritin in vivo. For healthy individuals, iron loading into serum ferritin can function in 1.0 mM phosphate levels if some H ferritin is present. However, CKD patients with elevated phosphate levels approaching 3.5 mM phosphate could have ferritin iron loading inhibited up to $\sim$ 50% resulting in the formation of the Fe(III)-phosphate complex. The Fe(III)-phosphate complex may contribute to the NTBI found in CKD patients and once formed is not a substrate for loading into ferritin. Perhaps a more significant discovery is that homopolymers of L ferritin were almost completely inhibited under intracellular phosphate concentrations (10 mM phosphate). These data infer that for ferritin to obtain iron in the cytosol, H ferritin is required for proper iron loading. For cells with predominantly L ferritin, an alternative mechanism that does not rely on Fe^{2+} diffusion may be required. This study suggests that iron-chaperones, such as the recently discovered PCBP1, may be an essential component for the delivery of iron to ferritin inside the cell.

Acknowledgment We thank Brigham Young University for support to fund this project.

References

Aitken-Rogers H, Singleton C, Lewin A, Taylor-Gee A, Moore GR, Le Brun NE (2004) Effect of phosphate on bacterioferritin-catalysed iron(II) oxidation. J Biol Inorg Chem 9(2):161–170

Arosio P, Ingrassia R, Cavadini P (2009) Ferritins: a family of molecules for iron storage, antioxidation and more. Biochim Biophys Acta 1790(7):589–599. doi:10.1016/j.bbagen.2008.09.004

Baker HM, Anderson BF, Baker EN (2003) Dealing with iron: common structural principles in proteins that transport iron and heme. Proc Natl Acad Sci U S A 100(7):3579–3583. doi:10.1073/pnas.0637295100

Bakker GR, Boyer RF (1986) Iron incorporation into apoferritin the role of apoferritin as a ferroxidase. J Biol Chem 261(28):13182–13185

Bates GW, Schlabach MR (1973) The reaction of ferric salts with transferrin. J Biol Chem 248(9):3228–3232

Bates GW, Schlabach MR (1975) The nonspecific binding of Fe^{3+} to transferrin in the absence of synergistic anions. J Biol Chem 250(6):2177–2181

Cheng YG, Chasteen ND (1991) Role of phosphate in initial iron deposition in apoferritin. Biochemistry 30(11):2947

Cohen LA, Gutierrez L, Weiss A, Leichtmann-Bardoogo Y, Zhang DL, Crooks DR, Sougrat R, Morgenstern A, Galy B, Hentze MW, Lazaro FJ, Rouault TA, Meyron-Holtz EG (2010) Serum ferritin is derived primarily from macrophages through a nonclassical secretory pathway. Blood 116(9):1574–1584. doi:10.1182/blood-2009-11-253815

De Domenico I, Ward DM, di Patti MC, Jeong SY, David S, Musci G, Kaplan J (2007) Ferroxidase activity is required for the stability of cell surface ferroportin in cells expressing GPI-ceruloplasmin. EMBO J 26(12):2823–2831. doi:10.1038/sj.emboj.7601735

De Domenico I, Vaughn MB, Paradkar PN, Lo E, Ward DM, Kaplan J (2011) Decoupling ferritin synthesis from free cytosolic iron results in ferritin secretion. Cell Metab 13(1):57–67. doi:10.1016/j.cmet.2010.12.003

de Silva D, Guo JH, Aust SD (1993) Relationship between iron and phosphate in mammalian ferritins. Arch Biochem Biophys 303(2):451–455

Di Marco GS, Hausberg M, Hillebrand U, Rustemeyer P, Wittkowski W, Lang D, Pavenstadt H (2008) Increased inorganic phosphate induces human endothelial cell apoptosis in vitro. Am J Physiol Renal Physiol 294(6): F1381–F1387. doi:10.1152/ajprenal.00003.2008

Evans RW, Rafique R, Zarea A, Rapisarda C, Cammack R, Evans PJ, Porter JB, Hider RC (2008) Nature of non-transferrin-bound iron: studies on iron citrate complexes and thalassemic sera. J Biol Inorg Chem 13(1):57–74. doi:10.1007/s00775-007-0297-8

Fiske CH, Subbarow Y (1925) The colorimetric determination of phosphorus. J Biol Chem 66(2):375–400

Friedman EA (2005) An introduction to phosphate binders for the treatment of hyperphosphatemia in patients with chronic kidney disease. Kidney Int 96:S2–S6

Granick S, Hahn PF (1944) Ferritin. VIII. Speed of uptake of iron by the liver and its conversion to ferritin iron. J Biol Chem 155(2):661–669

Harris WR (1986) Estimation of the ferrous-transferrin binding constants based on thermodynamic studies of nickel(II)-transferrin. J Inorg Biochem 27(1):41–52

Harris DC, Aisen P (1973) Facilitation of Fe(II) autoxidation by Fe(III) complexing agents. Biochim Biophys Acta 329(1): 156–158

Herbert V, Jayatilleke E, Shaw S, Rosman AS, Giardina P, Grady RW, Bowman B, Gunter EW (1997) Serum ferritin iron, a new test, measures human body iron stores unconfounded by inflammation. Stem Cells 15(4):291–296

Johnson JL, Cannon M, Watt RK, Frankel RB, Watt GD (1999) Forming the phosphate layer in reconstituted horse spleen ferritin and the role of phosphate in promoting core surface redox reactions. Biochemistry 38(20):6706–6713

Juan SH, Aust SD (1998) Iron and phosphate content of rat ferritin heteropolymers. Arch Biochem Biophys 357(2): 293–298

Kalantar-Zadeh K, Rodriguez RA, Humphreys MH (2004) Association between serum ferritin and measures of inflammation, nutrition and iron in haemodialysis patients. Nephrol Dial Transplant 19(1):141–149

Kalantar-Zadeh K, Kalantar-Zadeh K, Lee GH (2006) The fascinating but deceptive ferritin: to measure it or not to measure it in chronic kidney disease? Clin J Am Soc Nephrol 1(Supplement 1):S9–S18. doi:10.2215/cjn.01390406

Lee DH, Zacharski LR, Jacobs DR (2006) Comparison of the serum ferritin and percentage of transferrin saturation as exposure markers of iron-driven oxidative stress-related disease outcomes. Am Heart J 151 (6). doi:10.1016/j.ahj.2006.03.009

Levi S, Salfeld J, Franceschinelli F, Cozzi A, Dorner MH, Arosio P (1989) Expression and structural and functional properties of human ferritin L-chain from *Escherichia coli*. Biochemistry 28(12):5179–5184

Levi S, Santambrogio P, Corsi B, Cozzi A, Arosio P (1996) Evidence that residues exposed on the three-fold channels have active roles in the mechanism of ferritin iron incorporation. Biochem J 317(Pt 2):467–473

Lowry OH, Rosebrough NJ, Farr AL, Randall RJ (1951) Protein measurement with the folin phenol reagent. J Biol Chem 193(1):265–275

Malluche HH, Mawad H (2002) Management of hyperphosphataemia of chronic kidney disease: lessons from the past and future directions. Nephrol Dial Transplant 17(7):1170

Orino K, Kamura S, Natsuhori M, Yamamoto S, Watanabe K (2002) Two pathways of iron uptake in bovine spleen apoferritin dependent on iron concentration. Biometals 15(1):59–63

Paques EP, Paques A, Crichton RR (1980) A study of the mechanism of ferritin formation—the effect of ph, ionic-strength and temperature, inhibition by imidazole and kinetic-analysis. Eur J Biochem 107(2):447–453

Polanams J, Ray AD, Watt RK (2005) Nanophase iron phosphate, iron arsenate, iron vanadate, and iron molybdate minerals synthesized within the protein cage of ferritin. Inorg Chem 44(9):3203–3209

Prakash M, Upadhya S, Prabhu R (2005) Serum non-transferrin bound iron in hemodialysis patients not receiving intravenous iron. Clin Chim Acta 360(1–2):194–198

Ramanjaneyulu JVS, Shukla K (1956) Inorganic complexes in volumetric analysis—part II use of ferric phosphate complex in the estimation of iodide. Fresenius' Z Anal Chem 151(1):34–36

Rodriguez E, Simoes RV, Roig A, Molins E, Nedelko N, Slawska-Waniewska A, Aime S, Arus C, Cabanas ME, Sanfeliu C, Cerdan S, Garcia-Martin ML (2007) An iron-based T-1 contrast agent made of iron-phosphate complexes: in vitro and in vivo studies. Magn Reson Mater Phys Biol Med 20(1):27–37. doi:10.1007/s10334-006-0066-7

Samouilidou E, Grapsa E, Karpouza A, Lagouranis A (2007) Reactive oxygen metabolites: a link between oxidative stress and inflammation in patients on hemodialysis. Blood Purif 25(2):175–178

Santambrogio P, Levi S, Cozzi A, Rovida E, Albertini A, Arosio P (1993) Production and characterization of recombinant heteropolymers of human ferritin H and L chains. J Biol Chem 268(17):12744–12748

Santambrogio P, Levi S, Cozzi A, Corsi B, Arosio P (1996) Evidence that the specificity of iron incorporation into homopolymers of human ferritin L- and H-chains is conferred by the nucleation and ferroxidase centres. Biochem J 314(Pt 1):139–144

Shi H, Bencze KZ, Stemmler TL, Philpott CC (2008) A cytosolic iron chaperone that delivers iron to ferritin. Science 320(5880):1207–1210. doi:10.1126/science.1157643

Stenvinkel P, Barany P (2002) Anaemia, rHuEPO resistance, and cardiovascular disease in end-stage renal failure: links to inflammation and oxidative stress. Nephrol Dial Transplant 17(5):32–37

Sun S, Chasteen ND (1992) Ferroxidase kinetics of horse spleen apoferritin. J Biolo Chem 267(35):25160

ten Kate J, Wolthuis A, Westerhuis B, van Deursen C (1997) The iron content of serum ferritin: physiological

importance and diagnostic value. Eur J Clin Chem Clin Biochem 35(1):53–56

Tonelli M, Pannu N, Manns B (2010) Oral phosphate binders in patients with kidney failure. N Engl J Med 362(14): 1312–1324. doi:10.1056/NEJMra0912522

Treffry A, Harrison PM (1978) Incorporation and release of inorganic-phosphate in horse spleen ferritin. Biochem J 171(2):313–320

Wang W, Knovich MA, Coffman LG, Torti FM, Torti SV (2010) Serum ferritin: past, present and future. Biochim Biophys Acta 1800(8):760–769. doi:10.1016/j.bbagen.2010.03.011

Xu B, Chasteen ND (1991) Iron oxidation chemistry in ferritin. increasing Fe/O2 stoichiometry during core formation. J Biol Chem 266(30):19965

Yamanishi H, Iyama S, Yamaguchi Y, Kanakura Y, Iwatani Y (2002) Relation between iron content of serum ferritin and clinical status factors extracted by factor analysis in patients with hyperferritinemia. Clin Biochem 35(7):523–529

Yang X, Chasteen ND (1999) Ferroxidase activity of ferritin: effects of pH, buffer and Fe(II) and Fe(III) concentrations on Fe(II) autoxidation and ferroxidation. Biochem J 338(Pt 3):615–618

Yang X, Le Brun NE, Thomson AJ, Moore GR, Chasteen ND (2000) The iron oxidation and hydrolysis chemistry of *Escherichia coli* bacterioferritin. Biochemistry 39(16): 4915–4923